CrossMark

RESEARCH ARTICLE

Solar photocatalytic degradation of 2-chlorophenol with ZnO nanoparticles: optimisation with D-optimal design and study of intermediate mechanisms

Muneer M. Ba-Abbad[1,2,3] · Mohd S. Takriff[1,2] · Abdul Amir H. Kadhum[2] ·
Abu Bakar Mohamad[2,4] · Abdelbaki Benamor[5] · Abdul Wahab Mohammad[1,2]

Abstract In this study, the photocatalytic degradation of toxic pollutant (2-chlorophenol) in the presence of ZnO nanoparticles (ZnO NPs) was investigated under solar radiation. The three main factors, namely pH of solution, solar intensity and calcination temperature, were selected in order to examine their effects on the efficiency of the degradation process. The response surface methodology (RSM) technique based on D-optimal design was applied to optimise the process. ANOVA analysis showed that solar intensity and calcination temperature were the two significant factors for degradation efficiency. The optimum conditions in the model were solar intensity at 19.8 W/m^2, calcination temperature at 404 °C and pH of 6.0. The maximum degradation efficiency was predicted to be 90.5% which was in good agreement with the actual experimental value of 93.5%. The fit of the D-optimal design correlated very well with the experimental results with higher values of R^2 and R^2_{adj} correlation coefficients of 0.9847 and 0.9676, respectively. The intermediate mechanism behaviour of the 2-chlorophenol degradation process was determined by gas chromatography-mass spectrometry (GC-MS). The results confirmed that 2-chlorophenol was converted to acetic acid, a non-toxic compound.

Keywords 2-chlorophenol · Photocatalytic · ZnO NPs · D-optimal design

Responsible editor: Suresh Pillai

✉ Muneer M. Ba-Abbad
   muneer711@gmail.com

1   Research Centre For Sustainable Process Technology, Faculty of Engineering and Built Environment, Universiti Kebangsaan Malaysia, 43600 Bangi, Selangor, Malaysia

2   Department of Chemical and Process Engineering, Faculty of Engineering and Built Environment, Universiti Kebangsaan Malaysia, 43600 Bangi, Selangor, Malaysia

3   Department of Chemical Engineering, Faculty of Engineering and Petroleum, Hadhramout University of Science & Technology, Mukalla, Hadhramout, Yemen

4   Fuel Cell Institute, Universiti Kebangsaan Malaysia, 43600 Bangi, Selangor, Malaysia

5   Gas Processing Centre, Qatar University, P. O. Box 2713, Doha, Qatar

Introduction

Recently, chlorophenol compounds have been applied in many industries and have become one of the serious pollutants of water. These compounds are among the main pollutants released from industries such as petroleum refineries and pesticide manufacture (Lam et al. 2005). In addition, chlorophenol has been produced as a by-product from agricultural chemicals, synthetic resins and pulp and paper mills (Parida and Parija. 2006). The Environmental Protection Agency (EPA) has declared chlorophenols to be toxic to humans (US EPA 2006). These compounds were introduced into the ecological system through wastewater released from industrial plants. Traditional methods for the eradication of chlorophenols include biological and chemical treatments and these methods are saddled with disadvantages and limitations (Czaplicka 2006). Since the 1990s, it has been possible to remove chlorophenols completely from aqueous solutions with advanced oxidation processes (AOPs) using heterogeneous photocatalysis. Recently, the focus has been on the generation of highly reactive hydroxyl radicals ($^\bullet$OH)

on the surface of a photocatalyst because of their ability to destroy chlorophenols in water to produce a non-toxic product under ambient processing conditions (temperature and pressure) (Han et al. 2012). Photocatalysis has many advantages: (1) the reaction can take place at a low temperature (ambient temperature), (2) several organic pollutants can be degraded in both aqueous and gaseous systems, and (3) it is an inexpensive method for treating environmental contaminants (Demeestere et al. 2007). ZnO nanoparticles as a well-known photocatalyst have been applied to degrade toxic organic pollutants from water into innocuous materials in the presence of UV light (Venkatesham et al. 2012). ZnO nanoparticles are easily excited by UV light and then generate electron–hole pairs which then form $^\bullet OH$ and $^\bullet O^{2-}$ radicals (Ong et al. 2016). Several studies have been conducted to compare the activity of various semiconductors for photocatalytic activity and ZnO plays a vital role to become the best because it has good properties such as low cost, good optical and chemical properties and large absorbance of solar spectrum (Fenoll et al. 2013). The application of solar light in the photocatalytic process in countries with a suitable climate has been seen to be both trouble-free and economical. Solar light consisting of ultraviolet and visible light is free, environmentally friendly and a renewable source of energy (Ba-Abbad et al. 2013c).

The performance of photocatalytic degradation process depends on many general parameters such as photocatalyst dose, morphology of photocatalyst, initial concentration, pH of solution, light intensity and air flow rate etc. which needed to be carefully optimised. The traditional method to optimise the photocatalytic degradation process using one factor at a time is time consuming and expensive. There could be misinterpretation of results when there is interaction between the two process factors (Lin et al. 2009). To avoid these drawbacks, the useful tool of statistical design has been widely applied to optimise and predicate the process with interaction between several parameters as same time (Sin et al. 2011). According to literature, Response surface methodology (RSM) has been proven to be effective for the photocatalytic degradation process for wastewater treatment. RSM is a good statistical technique used for the design of experiments and the building of experimental models involving many interactive parameters. RSM is used to determine the effectiveness and robustness of a design according to the selection of more significant points from the general points for an adequate and satisfactory region of the design (Ba-Abbad et al. 2013a). Previous works have shown the use of RSM in many applications such as degradation of different pollutants and other industrial effluents field (Lin et al. 2009; Tao et al. 2009).

D-optimal design (D = dispersion matrix) fits these criteria sufficiently compared with other designs such as Central composite design and Box Behnken (Hasan et al. 2012). D-optimal design is one of the more popular and efficient ways to construct a quadratic model (Myers and Montgomery

2002). One of the advantages of this design is that the number of experiments is specified by the selection of certain points from a large set of candidate points. The best set of experimental points is maximised by the determinant $|X^T X|$|XTX|, in which the 'D' stands for the matrix determinant $|X^T X|$ related to the model. The maximum variance of the predicted responses of the process is minimised with D-optimal design, whereby the experimental points can minimise the error of the coefficients of the response model (Douglas 2009). In this study, D-optimal design was selected to optimise the photocatalytic degradation process of 2-chlorophenol in the presence of ZnO nanoparticles under solar radiation.

Experimental

Materials

The selected pollutant 2-chlorophenol (2-CP) was supplied by Merck. Hydrochloric acid and sodium hydroxide, obtained from Merck and R&M Chemicals respectively, were used to adjust pH solutions. Deionised water was used for preparing standard solutions of 2-CP. ZnO nanoparticles (ZnO NPs) were selected as the photocatalyst, which was prepared via the sol-gel method as in a previous study which include characterizations (Ba-Abbad et al. 2013b). The average particle sizes of ZnO NPs under different calcination temperatures of 400, 500 and 600 °C were found to be 20, 31 and 40 ± 2 nm, respectively.

Photocatalytic experimental procedures and analysis

All experiments relating to 2-CP degradation were carried out in a cylindrical slurry batch reactor. A certain amount of ZnO NPs was mixed with 100 ml of 2-CP solution (50 mg/L). The adsorption-desorption equilibrium between the ZnO NPs and 2-CP was achieved by dark stirring for 30 min. Then the mixture of ZnO NPs and 2-CP was exposed to direct solar radiation under different conditions (sunny, semi-cloudy and cloudy) to allow a reaction to take place. All experiments were run between the hours of 11.00 and 12.00 a.m. and ambient temperatures ranged from 30 to 38 °C. After 60 min of irradiation time, 1 mL of solution was analysed by high-performance liquid chromatography (HPLC) after centrifuging and filtering to remove the particles. The HPLC instrument of Agilent 1200 was applied to detect the concentration of 2-CP. A Jones LC-18 column (250 mm × 4.6 mm × 4 μm) with UV detector and acetonitrile: water (20:80 v/v) with 0.01 M phosphoric acid (H_3PO_4) with flow rate 1.0 ml min^{-1} was used as the mobile phase. However, 2 mL of 2-CP before and after degradation were withdrawn to determine the chemical oxygen demand (COD) removal. The standard calibration for 2-CP with R^2 correlation fit of 0.996

was evaluated. The degradation efficiency (DE%) and chemical oxygen demand (COD %) removal of 2-CP before and after degradation were measured by Eq. 1 and 2 below:

$$\text{Photocatalytic degradation } (DE\%) = \left(\frac{C_o - C_t}{C_o}\right) \times 100 \quad (1)$$

$$\text{COD removal} (COD\%) = \left(\frac{COD_o - COD_t}{COD_o}\right) \times 100 \quad (2)$$

where C_o, COD_0 (mg/L) are the initial concentration and chemical oxygen demand at $t = 0$ min, and C_t (mg/L), COD_t are the concentration and chemical oxygen demand of 2-CP solution after 60 min of irradiation time. At the same time, the COD% removal was carried out with the close reflux, colorimetric method using a HACH DR/2010 Spectrophotometer with COD reactor. The intermediate compounds within degradation of 2-CP were identified by gas chromatography-mass spectrometry (GC-MS) (Agilent 7890A–GC system). The GC-MS runs with a column of HP-5 measuring 30 m × 320 μm × 0.25 μm. The operation conduction, including of oven temperature started at 60 °C for 1 min, and then raise by 20 °C/min up to 300 °C with the injection volume of sample at 1 μL. The procedures of acetylation processes used to determine intermediate compounds were reported (Al-Janabi et al. 2012). The toxicity test of 2-CP before and after degradation under different irradiation time was investigated using *Escherichia coli* (*E. coli*) bacteria. *E. coli* bacteria were used as indicator strain and growth inhibition to determine the level of 2-CP and their intermediates compounds toxicity within degradation. For toxicity test, the agar disc diffusion method was applied as a good method as reported in the earlier study to reflect the toxicity levels of chlorophenols (Czaplicka 2006). The preparation of medium for *E. coli* bacteria's growth and all procedures to run toxicity test using agar disc diffusion method was reported previously (Ba-Abbad et al. 2016). Additionally, the average intensity of solar radiation (UVA spectra) for different weather conditions (sunny, semi-cloudy and cloudy days) was measured with a SkyeLynx type SDL 5100. Average intensity measurements were recorded every 15 min between 10.00 and 4.00 as shown in Fig. 1a. The average intensity of different conditions was 20, 15 and 10 W/m² for sunny, semi-cloudy and cloudy days respectively and was applied in this design at 11.00 and 12.00 a.m. (Fig. 1b).

Experimental design and optimisation of degradation process

Recently, RSM has been used in optimisation of many processes for different applications. The purpose is to create a good interaction effects between all the factors with reducing
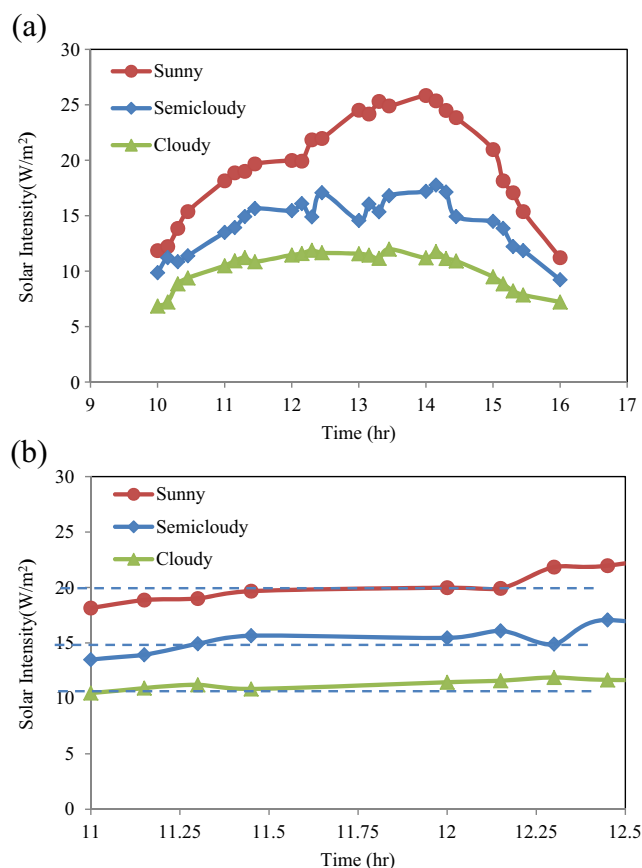

Fig. 1 Solar intensity under different conditions of sunny, semi-cloudy and cloudy days **a** wide time, **b** experiment time

of experiment runs and time consuming to other the classical process (Ba-Abbad et al. 2013a). All designs of RSM include mathematical correlation between processes factors were developed in the final model of process response which can be described by polynomial Eq. 3:

$$Y = \beta_o + \sum_{i=1}^{k} \beta_i X_i + \sum_{i=1}^{k} \beta_{ii} X^2_i + \sum_{1 \leq i \leq j}^{k} \beta_{ij} X_i X_{ij} + \varepsilon \quad (3)$$

For the process consisting of three factors, the best relationship between factors mathematically by second order equation was investigated as Eq. 4:

$$\begin{aligned} Y = \beta_o &+ \beta_1 X_1 + \beta_2 X_2 + \beta_3 X_3 + \beta_{11} X^2_1 \\ &+ \beta_{22} X^2_2 + \beta_{33} X^2_3 + \beta_{12} X_1 X_2 + \beta_{13} X_1 X_3 \quad (4) \\ &+ \beta_{23} X_2 X_3 \end{aligned}$$

where Y is the predicted response, X_1, X_2, X_3 are process factors, β_i is the coefficients, β_{ii} is coefficients of the quadratic terms, β_{ij} is the coefficients of the interactions of factors, ε is random error.

To complete the optimisation process, the factors were selected. Moreover, it has been reported that the highest surface area and optical properties of ZnO NPs help to test the photocatalytic degradation activity of the pollutant under direct solar irradiation (Pardeshi and Patil 2008). Many factors affects the photocatalytic process such as the pH of media solution, intensity of light, properties of the catalyst (such as particle size and surface area), which are influenced by the calcination temperature (Konstantinou and Albanis 2004; Vulliet et al. 2003). Temperature was not included in the design in this study because it can affect the adsorption and desorption of molecules. Although it has no significant effect on the rate of the photocatalytic reaction because in study very closed for all experimental condition (Ba-Abbad et al. 2012). On the other hand, a higher temperature leads to a reduction in the dissolved oxygen concentration in water, and the photocatalytic removal of pollutants from water under almost ambient conditions has been recommended (Ba-Abbad et al. 2015). For greater photocatalytic efficiency (DE), the Design Expert® software (Version 6.0, Stat Ease Inc.) based on the D-optimal design was used for the optimisation, as it saves material and time. The process factors together with their levels and codes for the optimisation of the photocatalytic process are given in Table 1.

Eighteen experimental runs based on D-optimal design with three factors (pH of solution, calcination temperature (°C) and solar intensity (W/m²)) with their levels were created and are given in Table 2. Analysis of variance (ANOVA) of photocatalytic degradation based on D-optimal design was applied to show the significant model and factors with interaction between all factors according to p value to produce optimum efficiency for the process. The p value is widely applied in statistical hypothesis testing. The p value ≤ 0.05 indicates that model or factor is significant and p value >0.05 indicates that that model or factor is not significant (Sin et al. 2011).

Results and discussion

Model fitting and ANOVA analysis

The results of the degradation efficiency (DE) and the removal of dissolved oxygen (COD) tested under different conditions were recorded and are presented in Table 2 together with a

Table 1 Parameters and their levels for optimization of photocatalytic process

Factor name	Factor	Levels		
	X_i	−1	0	+1
pH of solution	X_1	4	6	8
Calcination temperature (°C) of ZnO NP	X_2	400	500	600
Solar intensity (W/m²)	X_3	10	15	20

Table 2 Actual and predicted results of optimization based on D-optimal design with DE% and COD% responses

Std	Run no.	X_1	X_2	X_3	DE% (act.)	DE% (per.)	COD% (act.)	COD% (per.)
1	14	4	400	10	37.80	39.29	32.72	33.94
2	11	8	400	20	88.27	87.51	84.84	84.54
3	15	4	400	20	84.53	85.87	82.27	83.13
4	18	8	600	20	59.83	59.35	53.42	53.56
5	7	6	600	10	30.80	34.36	29.69	32.88
6	9	6	400	15	73.05	72.45	70.30	69.94
7	6	8	500	15	58.98	63.45	55.15	59.57
8	13	6	500	20	80.28	81.83	76.24	78.08
9	5	8	400	10	38.53	42.13	35.75	38.56
10	1	4	600	15	47.01	47.65	43.69	44.19
11	17	5	500	15	61.05	55.03	57.03	51.49
12	10	4	600	10	28.71	28.66	25.72	25.86
13	16	8	600	10	33.46	30.77	31.75	28.81
14	12	4	600	20	58.93	58.43	54.18	53.82
15	4	8	600	20	59.83	59.35	54.57	53.56
16	3	4	400	20	86.53	85.87	83.69	83.13
17	8	8	400	10	45.77	42.13	41.21	38.56
18	2	8	400	20	88.57	87.51	86.51	84.54

Actual act., *predicted* per

comparison with the predicted values. The DE and COD were found to be almost in agreement with the predicted values from the model. The results of the experiments based on the D-optimal design were analysed by ANOVA and the final regression equation for the responses was created for the model with factor codes as given in Eq. 5 and Eq. 6:

$$DE\ (\%) = -200.80058 + 15.30287X_1 + 0.47468X_2$$
$$+ 13.07128X_3 - 1.16098X^2_1 - 4.40184E{-}004X^2_2$$
$$- 0.16438X^2_3 - 9.01719E{-}004X_{12} - 0.030043X_{13}$$
$$- 8.4033E{-}003X_{23}$$

$$(5)$$

$$COD\ (\%) = -222.58805 + 19.42393X_1 + 0.45193X_2$$
$$+ 14.71225X_3 - 1.38626X^2_1 - 3.77796E{-}004X^2_2$$
$$- 0.17419X^2_3 - 2.08309E{-}003X_{12} - 0.080139X_{13}$$
$$- 0.010618X_{23}$$

$$(6)$$

Where, X_1 is pH of the solution, X_2 is the calcination temperature and X_3 is the solar intensity and X_{12}, X_{13} and X_{23} is the interaction between these factors. The ANOVA results of the

DE and COD models are summarised in Tables 3 and 4, respectively. The significance of all the factors is shown through the p value. The p value for each factor that is less than 0.05 (<0.050) is significant; any p value that is more than 0.05 (> 0.050) is not a significant factor for the model. The more significant factors were the calcination temperature (X_2) and solar intensity (X_3), with linear effects on the model. However, the pH of the solution (X_1) had no effect on the final response as the p value was greater than 0.05. The value of adequate precision was 21.116 and 22.519, for DE and COD, respectively, which is greater than the desirability value of four and indicates single adequacy (Korbahti and Rauf 2008). Moreover, the lack of fit was found to be 2.96 and 4.91 (F value), which is also insignificant compared with the pure error.

The regression models of the DE% and COD% responses were confirmed by the correlation coefficients of R^2 and R^2_{adj} values and Eqs. 5 and 6. For the model, the R^2 and R^2_{adj} values were 0.9847 and 0.9676 for the DE% compared with 0.9867 and 0.9717 for COD%, respectively. A very important step in the analysis of the results is the check on the adequacy of the model, whereby good adequacy indicates that the model is close to the real process. This can be expressed by comparing the actual and the predicted results of the DE% and the COD%, where R^2 gives the reduction in the variability of the response owed to the effects of the factors in the modelled process. A higher value of R^2 is not always good, and the desired R^2_{adj} that is also used for the model is not always higher. The results of R^2 and R^2_{adj} indicate that there was a good adequate approximation of the model to the actual values that resulted from the experiments (Chung et al. 2015).

Table 3 Analysis of variance (ANOVA) for the DE% of 2-CP

Source	Sum of squares	Degree of freedom	Mean square	F value	P value
Model	7218.73	9	802.08	57.37	<0.0001*
X_1	11.30	1	11.30	0.81	0.3948**
X_2	1336.19	1	1336.19	95.57	< 0.0001*
X_3	4523.99	1	4523.99	323.58	< 0.0001*
X^2_1	45.40	1	45.40	3.25	0.1092**
X^2_2	33.05	1	33.05	2.36	0.1627**
X^2_3	35.55	1	35.55	2.54	0.1495**
X_{12}	0.40	1	0.40	0.028	0.8706**
X_{13}	1.01	1	1.01	0.072	0.7951**
X_{23}	214.67	1	214.67	15.35	0.0044*
Residual	111.85	8	13.98		
Lack of fit	83.59	4	20.90	2.96	0.1593**
Pure error	28.26	4	7.07		
Total	7330.58	17			

*Significant at <0.05 % level

**Not significant, $R^2 = 0.9847$, $R^2_{adj} = 0.9676$, std. dev. = 3.74, mean = 58.98, C. V = 6.34, adeq precision = 21.116

Table 4 Analysis of variance (ANOVA) for the removal COD% of 2-CP

Source	Sum of squares	Degree of freedom	Mean square	F value	P value
Model	7242.73	9	804.75	65.85	<0.0001*
X_1	15.24	1	15.24	1.25	0.2965**
X_2	1324.36	1	1324.36	110.83	< 0.0001*
X_3	4378.60	1	4378.60	358.30	<0.0001*
X^2_1	64.72	1	64.72	5.30	0.0504*
X^2_2	24.35	1	24.35	1.99	0.1958**
X^2_3	39.92	1	39.92	3.27	0.1083**
X_{12}	2.11	1	2.11	0.17	0.6887**
X_{13}	7.17	1	7.17	0.59	0.4656**
X_{23}	342.64	1	342.64	28.04	0.0007*
Residual	97.76	8	12.22		
Lack of fit	81.23	4	20.31	4.91	0.0761**
Pure error	16.23	4	4.13		
Total	7340.50	17			

*Significant at <0.05% level

**Not significant, $R^2 = 0.9867$, $R^2_{adj} = 0.9717$, std. dev. = 3.50, mean = 55.45, C. V= 6.30, adeq. precision = 22.519

Adequacy of regression model

Some characteristics and diagnostic plots of the optimisation process based on the D-optimal design are presented in Fig. 2. All the points of the experiments appeared near the line, confirming that there was no problem with the model with good assumptions by the ANOVA results. These results were confirmed by the normal probability versus the studentised residual plots, as shown in Fig. 2a. The random scattering of the experimental points compared with the funnel-shaped pattern that was obtained indicates that the DE % response had an original observation of variance with no problem between the response and the factors, as given in Fig. 2b (Chung et al. 2015). Figure 2c exhibits the main characteristic to continue the model analysis is outlier in which indicated that good distribution of experiment points and none them out of the range. The actual value of the DE% compared with the predicted value of the model was evaluated by the value of R^2 and R^2_{adj} as plotted in Fig. 2d. Generally, these coefficients have been influenced by the insignificant factor that resulted from the ANOVA analysis when the range of the factors and the limited number of runs played a major role in increasing or decreasing the R^2 and R^2_{adj} values. The R^2 and R^2_{adj} values, which were 0.9847 and 0.9676, respectively, show that a good model was created to explain the optimisation conditions for the degradation process. The studentised residuals for the experimental runs are shown in Fig. 2e, which indicates how many standard deviations occurred in the actual result value that deviated from the predicted value. The value of the studentised residuals occurred at intervals between −3.5 to
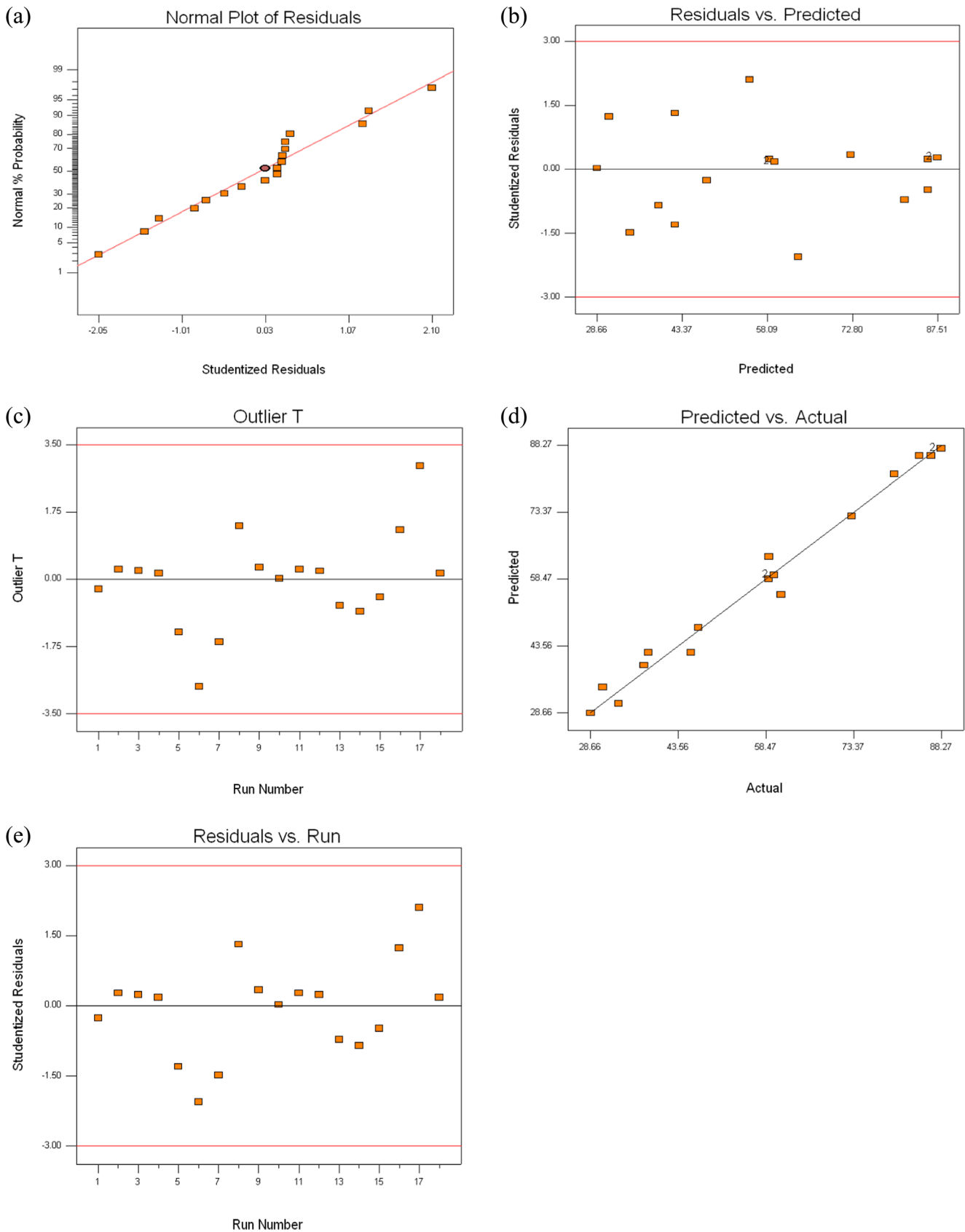
Fig. 2 Diagnostic plots of the degradation efficiency (DE%) for optimisation process, **a** normal probability, **b** studentised residual vs. predicted, **c** outlier, **d** actual vs. predicted, **e** studentised residuals vs. run

+3.5, and the observed response value was not respected for any value that was more or less than this value (Box et al. 2005). This model has values for the studentised residuals which are lower than ±3.5, which give a good fitting of the model to the response surface. The same effects of these factors on the COD % were observed.

Effect of factors on surface and counter plots

The effects of factors (pH of the solution, calcination temperature, and solar intensity) on the response surface and the contours of the DE% are presented in Fig. 3. These graphs help to explain the interaction between all the factors in optimising the conditions so as to maximise the required response. The same sequence of effects factors explanation on DE% will be also for COD% because the COD% removal had related to the DE% which indication by removal (degradation) of 2-CP from solution.

Effect of pH solution on degradation efficiency (DE%)

The effects of the pH of solution were semi-spherical, whereby the DE% increased at a pH of 6.0 and decreased when the pH was lower or higher than 6.0. This observation for both pH affects with calcination temperature and solar intensity as shown in Fig. 3a, b. Based on the earlier report, the pHzpc of ZnO is 9.0 and the surface of the catalyst is positive below pH of 9.0 and negative if the pH is more than 9.0 (Sakthivel et al. 2003). However, 2-CP exits as anions (negative charge) at pH < pKa (pKa of 2-CP = 8.52). DE% increase at pH of 6.0 could be attributed to more molecules of 2-CP being adsorbed on the ZnO NPs surface. However, the DE% decreased at pH ≈ pHzpc (pH at 8.0), and lower adsorption of 2-CP molecules on the ZnO surface occurred because of a less positive charge on the ZnO surface compared with pH of 6.0. At pH of 4.0, the DE% decreased because ZnO dissolved because of the amphoteric nature of the solution (Evgenidou et al. 2005; Musa et al. 2012). The maximum DE% of 2-CP was observed when the calcination temperature was at the lower level of 400 °C and solar intensity was at the higher level of 20 W/m^2 for pH of 6.0.

Effect of solar intensity on degradation efficiency (DE %)

The effects of solar intensity at the various values of calcination temperature and pH of solution are given in Fig. 3b, c. The DE% increased sharply from a minimum to a maximum intensity of 10–20 W/m^2 for cloudy and sunny days, respectively for both calcination temperature and pH. At the same time, a higher efficiency was found at a pH of 6.0 and calcination temperature at 400 °C for all solar intensities. The relationship between photocatalytic reaction rates and solar intensity was proportional, which indicated that the rate of the

reaction was limited by the intensity of the sunlight (Ram et al. 2011). Higher solar intensity leads to higher photon energy being absorbed on the surface of ZnO NPs which could be faster than electron recombination from valence band to conduction band. Many researchers have confirmed that increased DE% at higher photon energy causes an excess of photogenerated species such as e$^-$, h$^+$, $^\bullet$OH and $^\bullet$O$_2{}^-$ (Ahmed et al. 2011). Therefore, any decrease in intensity less than 20 W/m^2 (such as a sunny day) shows the clear influence on DE % of slower generation of e$^-$, h$^+$, $^\bullet$OH and $^\bullet$O$_2{}^-$ species.

Effect of calcination temperature of ZnO NPs on degradation efficiency (DE%)

Figure 3a, c shows the effects of the calcination temperature with both pH and solar intensities on the DE%. An increase in the DE% was observed with increases in the solar intensity and decreases in the calcination temperature at pH of 6.0. The calcination temperatures indicate the more significant factor effects on the surface area of ZnO NPs, which showed decreasing efficiency as temperature increased from 400 to 600 °C. The bigger particle and pore sizes of ZnO NPs have been reported as the main reason for decreases of surface area within the calcination process (Seetawan et al. 2011). DE% decreased when calcination temperature increased from 400 to 600 °C because lower molecules of 2-CP were adsorbed on the lower surface area of ZnO NPs (Hairom et al. 2014; Grcic et al. 2010). The most factors affecting DE% when calcination temperature interacts with solar intensity whereby higher efficiency of 91.3% was produced. These results were confirmed by the ANOVA analysis of individual and interaction p values for calcination temperature and solar intensity (Table 3).

According to the factor results, the calcination temperature and solar intensity have the main effects on DE%. The individual and interaction effects (two-factor) of these factors are presented in Fig. 4. The highest value of the DE % as the optimum conditions were observed when the calcination temperature and solar intensity at lower (400 °C) and high values (20 W/m^2), respectively as shown in Fig. 4a, b. However, the negative effects of these factors on DE% (in the polynomial expression, $X^2{}_2$, $X^2{}_3$) when higher calcination temperature and lower of solar intensity were reported within experiments. Nevertheless, the overall interaction effects showed higher influence on DE % which was confirmed by significant interaction (p value of $X_{23} < 0.050$) between calcination temperature and solar intensity, as given in Table 3. This effect on DE % was shown clearly when calcination temperature and solar intensity were combined together as given in Fig. 4c for experimental data. Additionally, the same sequences for the effects of these factors were obtained for the chemical oxygen demand (COD%) in all the experimental results.
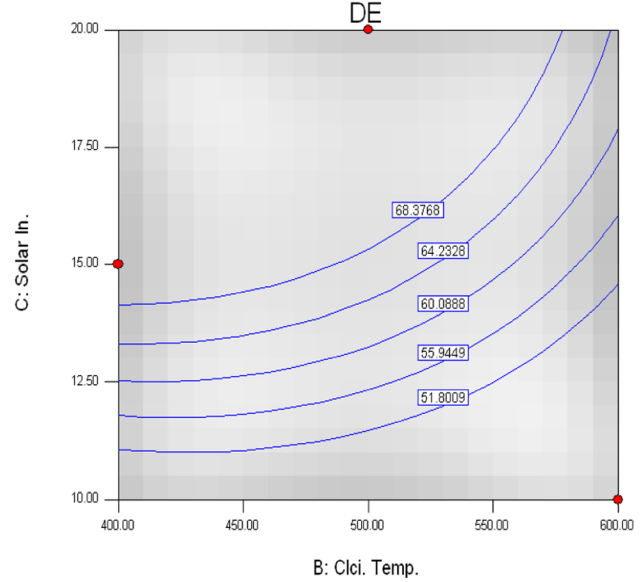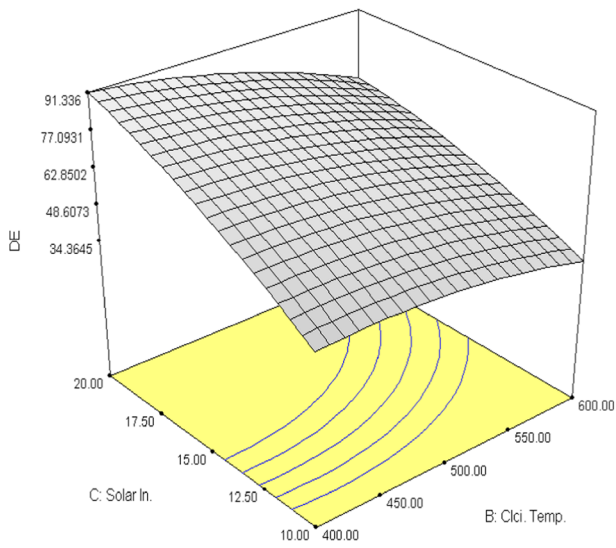
(a)
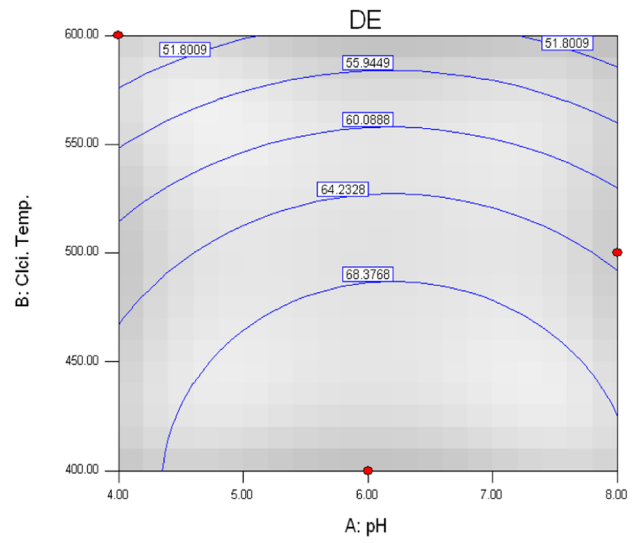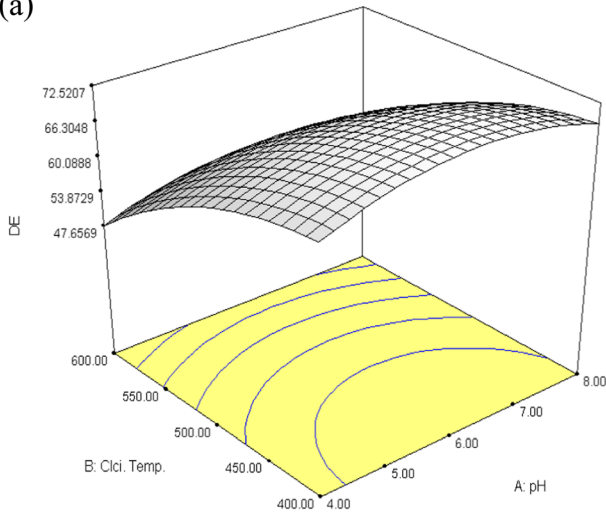
(b)
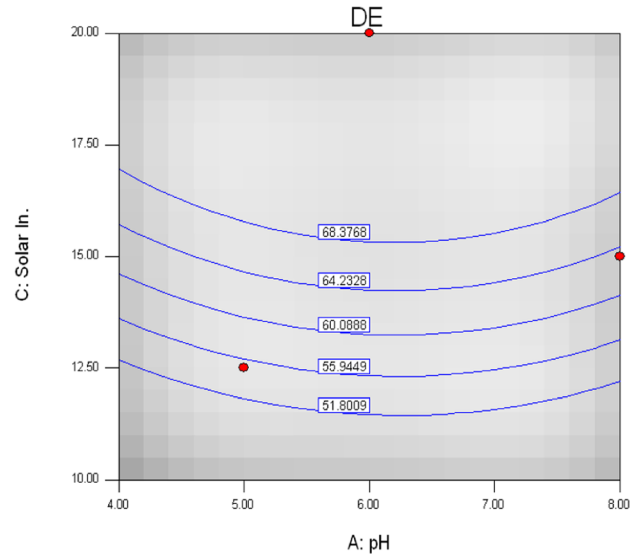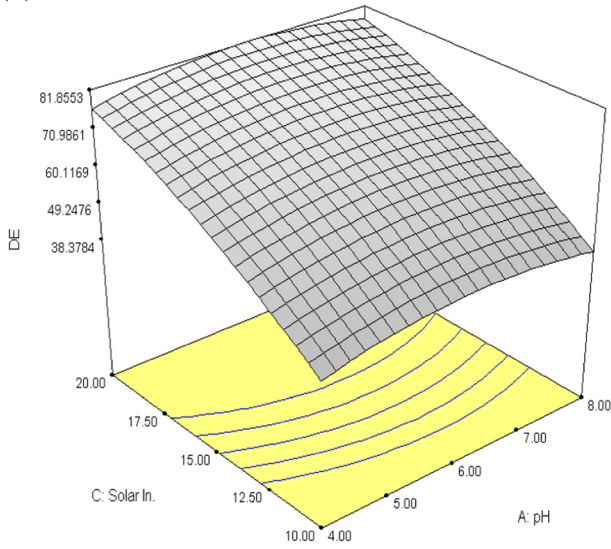
(c)

◀ **Fig. 3** Response surface and contour graphs of degradation efficiency (DE%) with effect on the process factors, **a** calcination temperature and pH, **b** solar intensity and pH, **c** solar intensity and calcination temperature

This process focuses on the generation of highly reactive hydroxyl radicals ($^{\bullet}$OH) on the surface of a photocatalyst because of their ability to destroy CPs in water to produce a non-toxic product under ambient processing conditions (temperature and pressure) [29]. The main factors of calcination temperature and solar intensity had more influence on the DE% in this study. This was because of the higher surface area of ZnO catalyst at optimum calcination temperature attributed to more 2-CP being adsorbed into that surface. Moreover, higher energy absorbed on a sunny day leads to an accelerated reaction on the surface of the ZnO catalyst (Ba-Abbad et al. 2013d). In addition, ZnO is absorbed, the energy increases to more than the band gap (3.2 eV) and a strongly reactive species is generated. The excitation of the electron (e^-) from the valence band to the conduction band generates holes in the valence band (h^+). Sequentially, the anion radicals ($O_2^{\bullet-}$) produced

from the electron react with the oxygen adsorbed on the catalyst surface and the hydroxyl radicals (OH$^{\bullet}$) from the hydroxide anions (OH$^-$) with holes (Hayat et al. 2011). The oxidation pathway mechanism of ZnO for the generation of the strong reactive radicals is as below:

$$ZnO + h\upsilon(\text{UVA of solar light with } \lambda < 388 \text{ nm}) \rightarrow e^- + h^+ \quad (7)$$

$$O_2 + e^- \rightarrow O_2^{\bullet-} \quad (8)$$

$$O_2^{\bullet-} + H^+ \rightarrow HO_2^{\bullet} \quad (9)$$

$$HO_2^{\bullet} + e^- \rightarrow HO_2^{-} \quad (10)$$

$$HO_2^{-} + H^+ \rightarrow H_2O_2 \quad (11)$$

$$H_2O_2 + e^- \rightarrow OH^{\bullet} + OH^- \quad (12)$$

$$H_2O + h^+ \rightarrow OH^{\bullet} + H^+ \quad (13)$$

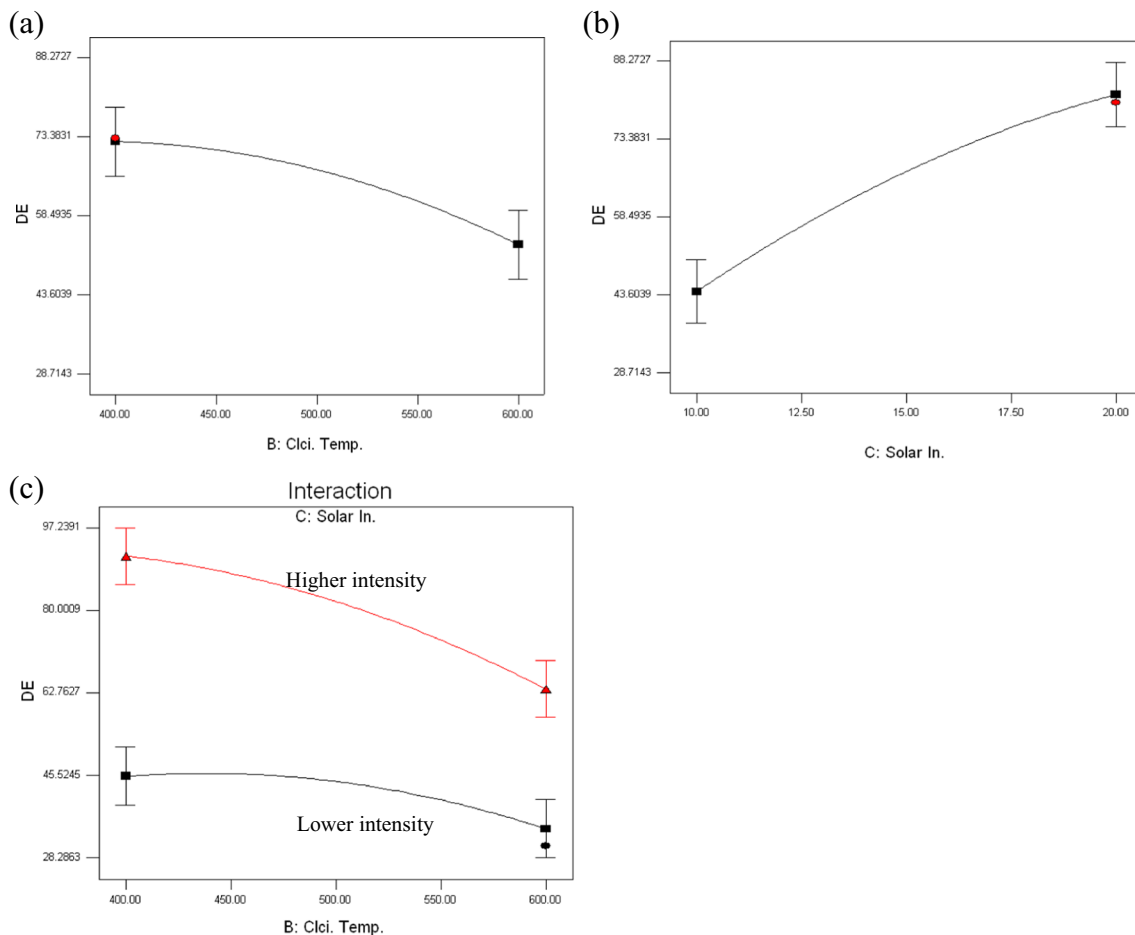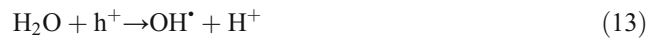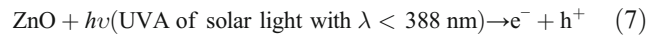$$OH^- + h^+ \rightarrow OH^{\bullet} \quad (14)$$

Fig. 4 Plots of main factors' effect on degradation efficiency (DE%), **a** calcination temperature, **b** solar intensity, **c** interactions between calcination temperature and solar intensity

Table 5 Experimental run and optimum conditions of all factors under range to maximise DE% and COD% for 2-CP

Run	pH	Calcination temperature (°C)	Solar intensity (W/m²)	DE% (predicted)	COD% (predicted)	DE% (actual)	COD% (actual)
1	6.08	404.29	19.76	90.430	88.356	93.47	88.98
2	6.09	411.50	23.00	97.803	95.581	99.54	97.57

Optimisation and model validation

According to the results from the model, the optimum conditions for maximum degradation efficiency were created. The main target of numerical optimisation based on D-optimal design was to maximise the desirability function to produce more accurate results (DE% and COD%). The software has

five options: maximum, minimum, target, in the range and equal to, which goal of optimisation put all factors was in is in the range and response of DE%, COD% in is maximum. The optimum values for all the factors from the model were generated to produce the maximum values of DE% and COD% and were coded as the first run shown in Table 5 and Fig. 5a. To validate the process model, the experiment
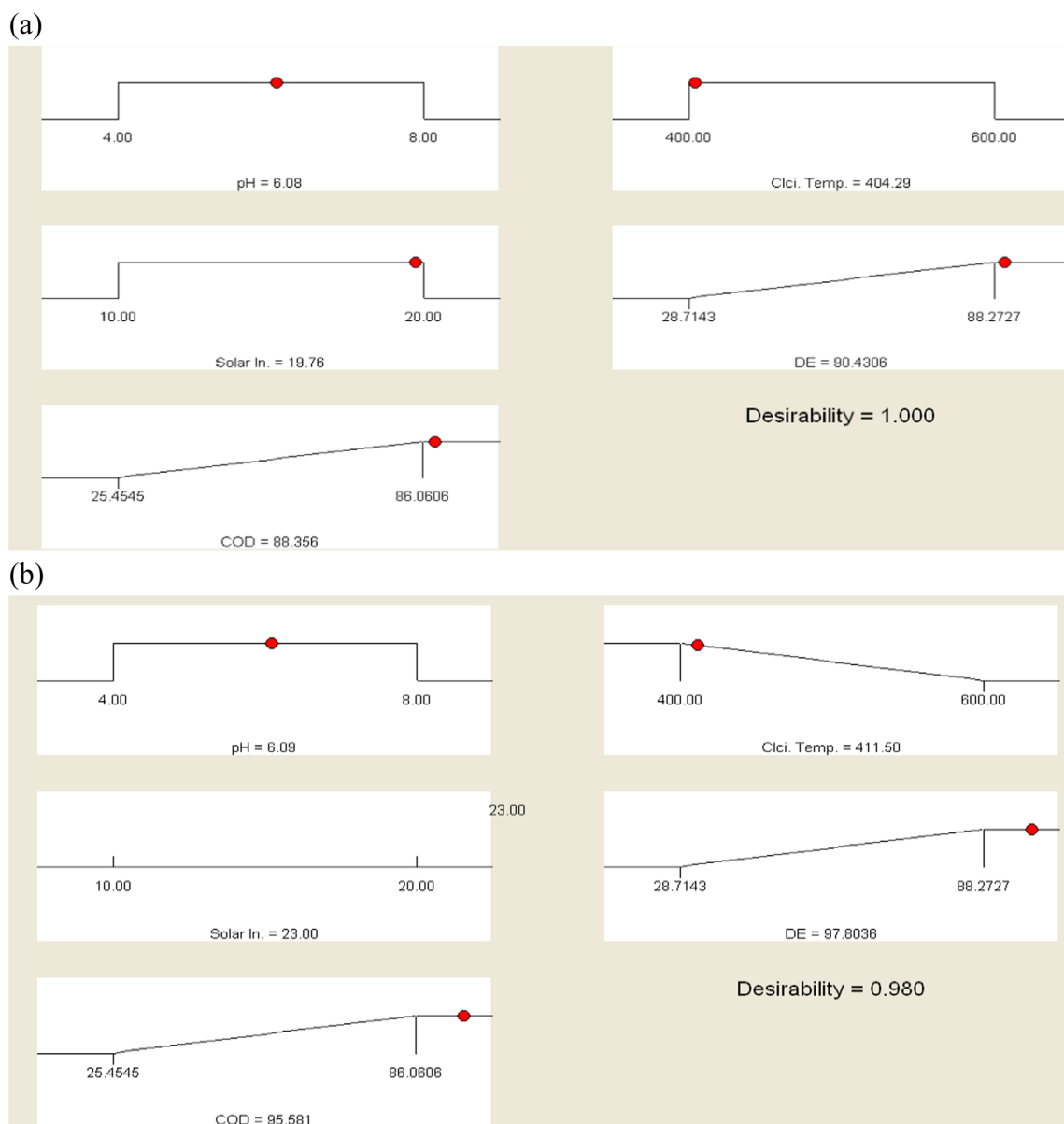

Fig. 5 Optimum conditions for maximum values of DE% and CO% with their desirability, **a** first run, **b** second run
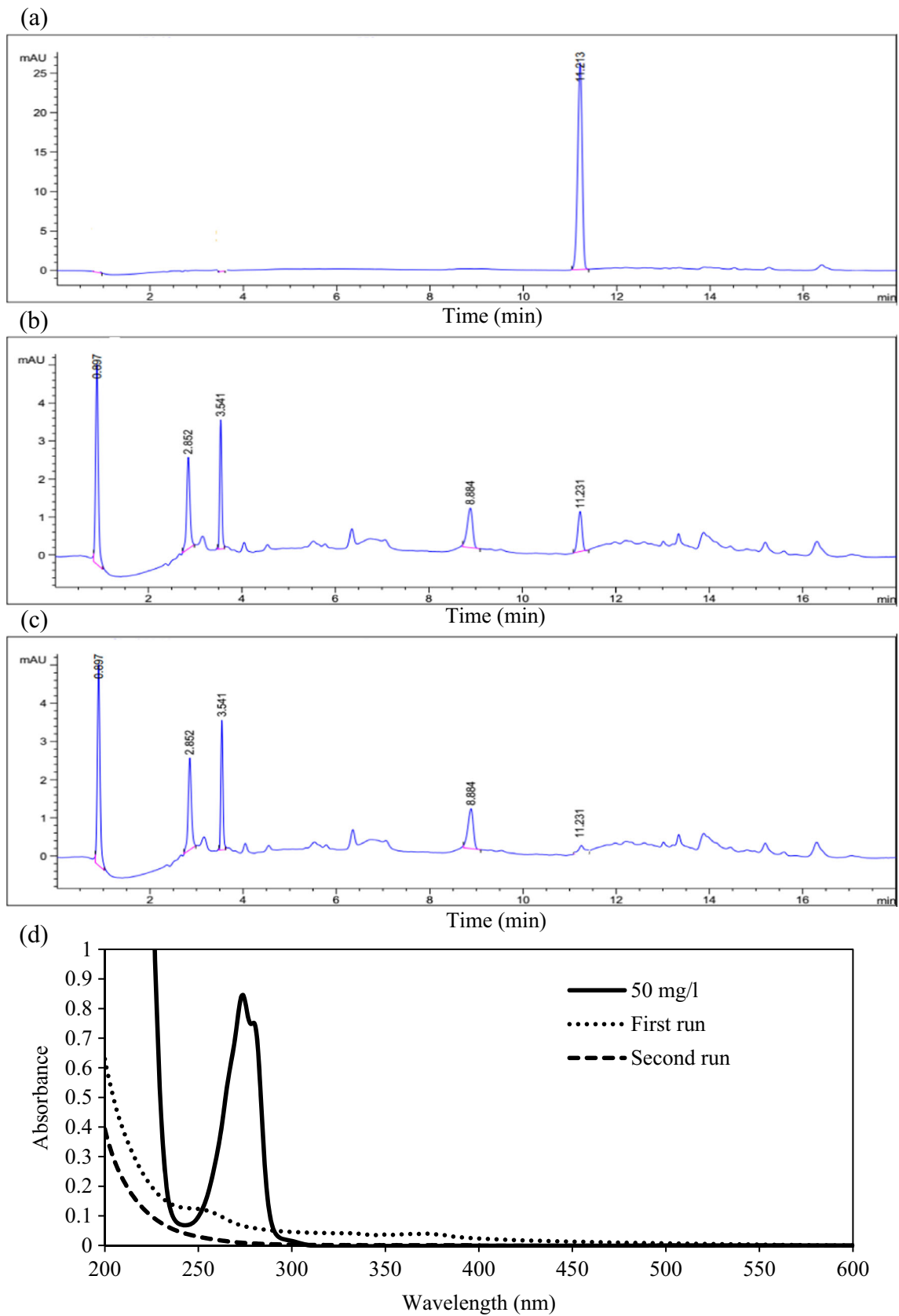
Fig. 6 Analysis of photocatalytic degradation with HPLC and UV, **a** 2-CP before reaction, **b** first run by HPLC, **c** second run by HPLC, **d** first and second run by UVvis

was run with the same values of the predicted conditions for all the factors. A good agreement between the DE% and COD% regarding the actual values and the predicted values was observed.

To validate the process model further, the second run was applied and adjusted with all the factors under the range when the solar intensity was 23 W/m^2 (equal to) as shown in Table 5 and Fig. 5b. This intensity value was measured between 12.00 and 14.30 (Fig. 1) to investigate the effects under real conditions and to determine the best time to achieve the maximum DE%. The highest DE% was found to be 97.803% compared with 99.54 % from the experiments, with a higher removal of COD%. The DE% of 2-CP under the optimisation conditions was confirmed by the HPLC and UV analysis as shown in Fig. 6. A single peak of the HPLC and UV analysis was obtained at the retention time of 11.2 min and wavelength of 274 nm, respectively for 50 mg/l before the degradation reaction in the presence of the ZnO NPs. After 60 min of exposure to direct solar radiation for the first run of optimisation, that peak was decreased based on the percentage of degradation compared to the second run of the experiment as presented in Fig. 6b, c. These results were confirmed by spectrophotometry as shown in Fig. 6d for first and second runs.

Intermediate mechanism study

Photocatalytic degradation of 2-CP by ZnO NPs was investigated with small molecules as intermediate compounds. These compounds were determined with GC-MS as shown in Fig. 7.

Table 6 Retention time of *2-CP* and intermediate compounds by GC-MS analysis with their molecular weight

NO.	Compounds name	Retention time of GC-MS (min)	Molecular weight (g mol^{-1})
1	2-chlorophenol	5.48	128
2	Phenol	4.139	94
3	Catechol	6.72	110
4	Hydroquinone (HQ)	6.56	110
5	hydroxyhydroquinone (HHQ)	8.012	127
6	2-chlorohydroquinone (CHQ)	6.072	145
7	Fumaric acid	4.53	119
8	Maleic acid	4.53	119
9	Acetic acid	–	60
10	Oxalic acid	5.92	90

The main intermediate compounds for all chlorophenols using GC-MS were found to be phenol, catechol, hydroquinone, chlorohydroquinone (CHQ), hydroxyhydroquinone (HHQ), carbon dioxide and water, as confirmed by previous studies (Rao et al. 2003). The main compounds with their retention time and molecular weight are summarised in Table 6.

All of the characteristic masses (*m/z*) of 2-CP and intermediates were in agreement with the molecular weight of their compounds. At the same time, characteristic masses (*m/z*) of hydroxyhydroquinone (HHQ), 2-chlorohydroquinone (CHQ), acetic acid and oxalic acid were slightly different from
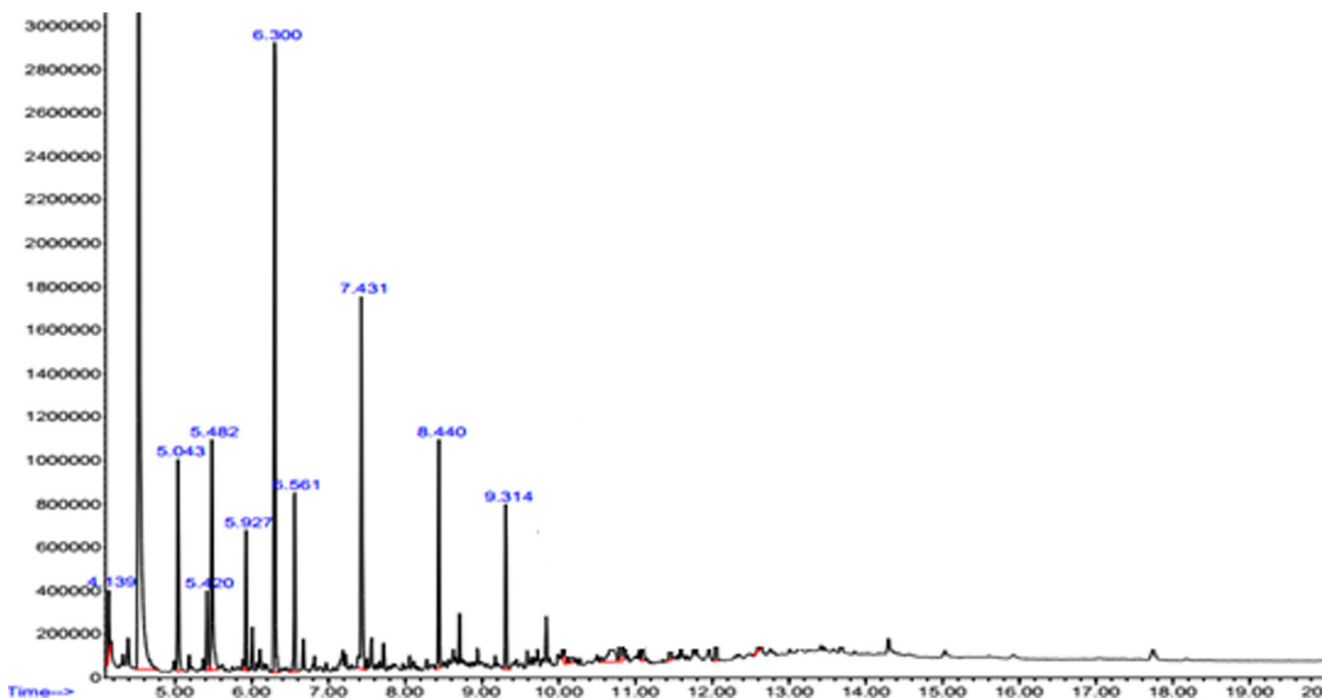

Fig. 7 GC-MS chromatogram of intermediate compounds within degradation process of 2-CP under optimum conditions in presence of ZnO NP

theoretical molecular weight (± 5) possibly because that compound has secondary characteristic masses (m/z) or low concentration and was converted faster to carbon dioxide within the long reaction time. From these data, it can be suggested that the pathway of the 2-CP degradation mechanism using ZnO NPs, as shown in Fig. 8. After the catalyst absorbed the

photons from solar light, highly reactive radicals of $^\bullet OH$ and $^\bullet \bar{O}_2$ were generated. The $^\bullet OH$ radical attacked the ortho-position and removed the Cl group, replacing it with $^\bullet OH$ to produce catechol ($m/z = 111$). The phenol ($m/z = 94$) was formed by loss of the OH group from catechol (mechanism, MI). The hydroxyhydroquinone (HHQ) was detected by GC-

Fig. 8 Pathway fragmentation of 2-CP degradation under optimum conditions in presence of ZnO NP

$CO_2 + CH_3 + H_2O$, COOH and HOCl
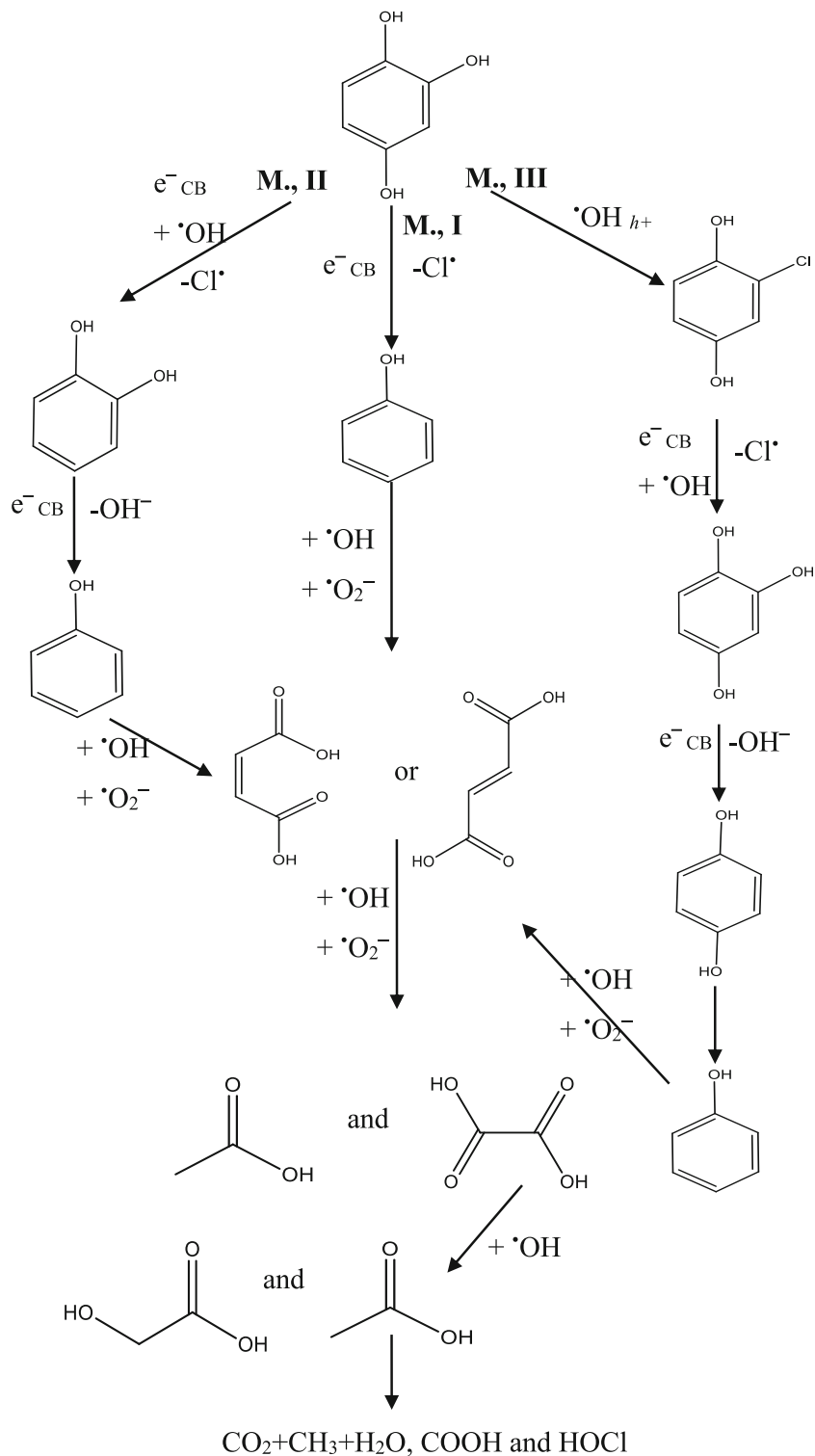
MS ($m/z = 127$) produced by the attack of two ortho- and para-position of 2-CP. In the ortho-position, the Cl group was removed by electrons on conduction band (e^-_{CB}) and para-position attacked by the $^\bullet$OH radical. The loss of the OH group from hydroxyhydroquinone generated catechol ($m/z = 111$) and phenol ($m/z = 94$) (mechanism, MII). The 2-chlorohydroquinone (CHQ) ($m/z = 141$) as the main compound of 2-CP fragmentation by attacks of the $^\bullet$OH para-position was found. The sequence of reactions formed hydroxyhydroquinone (HHQ) by attacking the electrons of the Cl group and replacing it with the OH group. However, losing of the OH group on para-position and then ortho-position, the catechol ($m/z = 111$) and phenol ($m/z = 94$) were produced (mechanism, MIII). In the three mechanisms suggested, the final product was phenol ($m/z = 94$) with a slight change (± 5) of fragmentation characteristic masses (m/z) from hydroxyhydroquinone (HHQ), 2-chlorohydroquinone (CHQ) due to the reactions. The $^\bullet$OH radical preferentially attacked the aromatic ring of phenols because of their electrophilic nature (Rao et al. 2003). This led to the formation of maleic and fumaric acid ($m/z = 119 \pm 5$) which were converted to smaller molecular compounds. The lower molecular compounds of final fragmentation were found to be oxalic acid ($m/z = 90 \pm 5$) and these were then converted to acetic acid hydroxyl ($m/z = 77 \pm 5$), acetic acid ($m/z = 60 \pm 5$), formic acid ($m/z = 46$), CO_2 ($m/z = 44$), COOH ($m/z = 45$) and CH_3 ($m/z = 15$) as reported in many studies (Bandara et al. 2001).

Toxicity test

Degradation of 2-CP under optimum conditions of solar intensity, pH and calcination temperature of ZnO was confirmed by the toxicity test. The toxicity of 2-CP before and after degradation was evaluated by inhibition zone method of bacteria growth for different irradiation time. The values of E. coli zone inhibition under different irradiation time of degradation were shown in Fig. 9. The values of inhibitions indicated higher toxicity of 2-CP before degradation. The toxicity of 2-CP is indicated by increasing lipophilicity that results to

higher potential of uptake into the organism. This phenomena leads to inhibition of bacteria growth (proliferate) increasing as reported by Czaplicka (2006). After 60 min of irradiation time, the inhibition zone was decreased to smaller area because almost 2-CP and intermediates compounds were converted to non-toxic by-products such as CO_2 and some acids (acetic and oxalic acids), according to the HPLC and GC-MS analysis in Figs. 6, 7, 8. Moreover, lower inhibition indicates after 60 min of irradiation time compare to before degradation (0 min) which due to close higher degradation efficiency. However, smaller zone of inhibition (0.07 mm) after degradation time of 60 min was attributed to effects of acetic acid as final by-product on E. coli growth as reported earlier (Roe et al. 2002).

Conclusions

Optimisation of the 2-chlorophenl degradation process was investigated to ascertain the main factors affecting efficiency (DE%) and oxygen demand removal (COD%). RSM based on D-optimal design was applied to optimise the process factors of pH of solution, solar intensity and calcination temperature. According to ANOVA analysis, degradation efficiency is more sensitive to solar intensity and calcination temperature. The final model of the optimisation process showed higher accuracy in predicting DE% and COD% results than the experimental model. The results showed good fitting of the D-optimal design model which was 0.9847, 0.9676 (DE%) and 0.9867, 0.9717 (COD%) for both R^2 and R^2_{adj} correlation coefficients, respectively. Finally, RSM based on D-optimal design for 2-chlorophenl degradation is a good statistical tool and gives suitable results for the maximum value of DE% and COD% within the optimisation process. The pathway of 2-chlorophenl degradation to the non-toxic intermediate compound acetic acid was investigated by gas chromatography-mass spectrometry (GC-MS).

Fig. 9 **a** Toxicity test of 2-CP degradation using agar disc diffusion. **b** Inhibition zone of growth, under different irradiation time using optimum conditions of process in presence of ZnO NP (initial concentration of 2-CP = 50 mg/l)
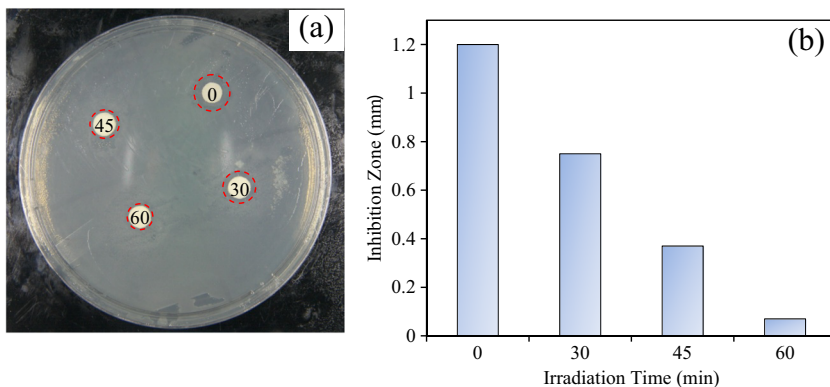
References

Ahmed S, Rasul MG, Brown R, Hashib MA (2011) Influence of parameters on the heterogeneous photocatalytic degradation of pesticides and phenolic contaminants in wastewater: a short review. J Environ Manag 92:311–330

Al-Janabi KS, Alazawi FN, Mohammed MI, Kadhum AH, Mohamad AB (2012) Direct acetylation and determination of chlorophenols in aqueous samples by gas chromatography coupled with an electron-capture detector. J Chromatogr Sci 50:564–568

Ba-Abbad MM, Takriff MS, Mohammad AW (2016) Enhancement of 2-chlorophenol photocatalytic degradation in the presence Co^{2+}-doped ZnO nanoparticles under direct solar radiation. Res Chem Intermed 42:52119–55236

Ba-Abbad MM, Chai PV, Takriff MS, Benamor A, Mohammad AW (2015) Optimization of nickel oxide nanoparticle synthesis through the sol–gel method using Box–Behnken design. Mater Des 86:948–956

Ba-Abbad MM, Kadhum AAH, Mohamad AB, Takriff MS, Sopian K (2013d) Photocatalytic degradation of chlorophenols under direct solar radiation in the presence of ZnO catalyst. Res Chem Intermed 39:1981–1996

Ba-Abbad MM, Kadhum AH, Mohamad AB, Takriff MS, Sopian K (2012) Synthesis and catalytic activity of TiO_2 nanoparticles for photochemical oxidation of concentrated chlorophenols under direct solar radiation. Inter J Electrochem Sci 7:4871–4888

Ba-Abbad MM, Kadhum AH, Mohamad AB, Takriff MS, Sopian K (2013a) Optimization of process parameters using D-optimal design for synthesis of ZnO nanoparticles via sol–gel technique. J Ind Eng Chem 19:99–105

Ba-Abbad MM, Kadhum AH, Mohamad AB, Takriff MS, Sopian K (2013b) The effect of process parameters on the size of ZnO nanoparticles synthesized via the sol–gel technique. J Alloys Compd 550:63–70

Ba-Abbad MM, Kadhum AH, Mohamad AB, Takriff MS, Sopian K (2013c) Visible light photocatalytic activity of Fe^{3+}-doped ZnO nanoparticle prepared via sol–gel technique. Chemosphere 91:1604–1611

Bandara J, Mielczarski JA, Lopez A, Kiwi J (2001) 2. Sensitized degradation of chlorophenols on iron oxides induced by visible light: comparison with titanium oxide. Appl Catal B 34:321–333

Box J, Hunter S, Hunter WG (2005) Statistics for experimenters: design, innovation, and discovery, 2nd edn. John Wiley & Sons, Inc., Hoboken

Chung YT, Ba-Abbad MM, Mohammad AW, Hairom NH, Benamor A (2015) Synthesis of minimal-size ZnO nanoparticles through sol–gel method: Taguchi design optimization. Mater Des 87:780–787

Czaplicka M (2006) Photo-degradation of chlorophenols in aqueous solution. J Hazard Mater 134:45–59

Demeestere K, Dewulf J, Langenhove H (2007) Heterogeneous photocatalysis as an advanced oxidation process for the abatement of chlorinated, monocyclic aromatic and sulfurous volatile organic compounds in air: state of the art. Crit Rev Env SciTechnol 37:489–538

Douglas CM (2009) Design and analysis of experiments, 7th edn. John Wiley & Sons, New York

Evgenidou E, Fytianos K, Poulios I (2005) Semiconductor-sensitized photodegradation of dichlorvos in water using TiO_2 and ZnO as catalysts. Appl Catal B 59:81–89

Fenoll J, HelIin P, Flores P, MartInez CM, Navarro S (2013) Degradation intermediates and reaction pathway of carbofuran in leaching water using TiO_2 and ZnO as photocatalyst under natural sunlight. J Photochem Photobiol A 251:33–40

Grcic I, Vujević D, Koprivanac N (2010) The use of D-optimal design to model the effects of process parameters on mineralization and discoloration kinetics of Fenton-type oxidation. Chem Eng J 157:408–419

Hairom NH, Mohammad AW, Kadhum AA (2014) Effect of various zinc oxide nanoparticles in membrane photocatalytic reactor for Congo red dye treatment. Sep Purif Technol 137:74–81

Han J, Liu Y, Singhal N, Wang L, Gao W (2012) Comparative photocatalytic degradation of estrone in water by ZnO and TiO_2 under artificial UVA and solar irradiation. Chem Eng J 213:150–162

Hasan DB, Abdul Aziz AR, Daud WM (2012) Using D-optimal experimental design to optimise remazol black B mineralisation by Fenton-like peroxidation. Enviro Technol 33:1111–1121

Hayat K, Gondal MA, Khaled MM, Ahmed S, Shemsi AM (2011) Nano ZnO synthesis by modified sol gel method and its application in heterogeneous photocatalytic removal of phenol from water. Appl Catal A 393:122–129

Konstantinou IK, Albanis TA (2004) TiO_2-assisted photocatalytic degradation of azo dyes in aqueous solution: kinetic and mechanistic investigation. Appl Catal B Environ 49:1–14

Korbahti BK, Rauf MA (2008) Response surface methodology (RSM) analysis of photoinduced decoloration of toludine blue. Chem Eng J 136:25–30

Lam SW, Chiang K, Lim TM, Amal R, Low GC (2005) Effect of charge trapping species of cupric ions on the photo catalytic oxidation of resorcinol. Appl Catal B 55:23–132

Lin YX, Ferronato C, Deng NS, Wu F, Chovelon JM (2009) Photocatalytic degradation of methylparaben by TiO_2: multivariable experimental design and mechanism. Appl Catal B 88:32–41

Musa AY, Ba-Abbad MM, Kadhum AAH, Mohamad AB (2012) Photodegradation of chlorophenolic compounds using zinc oxide as photocatalyst: experimental and theoretical studies. Res Chem Intermed 38:995–1005

Myers RH, Montgomery DC (2002) Response surface methodology, process and products optimization using designed experiments. John Wiley & Sons, Inc., New York

Ong CB, Mohammad AW, Rohani R, Ba-Abbad MM, Hairom NH (2016) Solar photocatalytic degradation of hazardous Congo red using low-temperature synthesis of zinc oxide nanoparticles. Process Saf Environ Prot. doi:10.1016/j.psep.2016.04.006

Pardeshi SK, Patil AB (2008) A simple route for photocatalytic degradation of phenol in aqueous zinc oxide suspension using solar energy. Sol Energy 82:700–705

Parida KM, Parija S (2006) Photocatalytic degradation of phenol under solar radiation using microwave irradiated zinc oxide. Sol Energy 80:1048–1054

Ram M, Andreescu ES, Hanming D (2011) Nanotechnology for environmental decontamination. McGraw Hill Professional, New York City

Rao NN, Dubey AK, Mohanty S, Khare P, Jain R, Kaul SN (2003) Photocatalytic degradation of 2-chlorophenol: a study of kinetics, intermediates and biodegradability. J Hazard Mater 101:301–314

Roe AJ, O'ByrneŒ C, McLaggan D, Booth IR (2002) Inhibition of *Escherichia coli* growth by acetic acid: a problem with methionine biosynthesis and homocysteine toxicity. Microbiology 148:2215–2222

Sakthivel S, Neppolian B, Shankar MV, Arvindo B, Palanichamy M, Murugesan V (2003) Solar photocatalytic degradation of azo dye: comparison of photocatalytic efficiency of ZnO and TiO_2. Sol Energy Mater Sol Cells 77:65–82

Seetawan U, Jugsujinda S, Seetawan T, Euvananont C, Junin C, Thanachayanont C, Chainaronk P, Amornkitbamrung V (2011) Effect of annealing temperature on the crystallography, particle size and thermopower of bulk ZnO. Solid State Sci 13:1599–1603

Sin JC, Lam SM, Mohamed A (2011) Optimizing photocatalytic degradation of phenol by TiO2/GAC using response surface methodology. Korean J Chem Eng 28:84–92

Tao YG, Ye LB, Pan J, Wang YM, Tang B (2009) Removal of Pb (II) from aqueous solution on chitosan/TiO$_2$ hybrid film. J Hazard Mater 161:718–722

US EPA (2006) National emission standards for hazardous air pollutants: miscellaneous organic chemical manufacturing. United States Environmental Protection Agency

Venkatesham V, Gattumane MM, Suggala VS, Halugondanahalli SP (2012) Photocatalytic degradation of methylene blue using a zinc oxide-cerium oxide catalyst. Eur J Chem 3: 191–195

Vulliet E, Chovelon JM, Guillard C, Herrmann JM (2003) Factors influencing the photocatalytic degradation of sulfonylurea herbicides by TiO$_2$ aqueous suspension. J Photochem Photobiol A 159: 71–79